Advanced Materials Research Vols. 433-440 (2012) pp 2092-2098
© (2012) Trans Tech Publications, Switzerland
doi:10.4028/www.scientific.net/AMR.433-440.2092

Dynamic Sliding Mode Control of Air-to-fuel ratio in Internal Combustion Engines Using the Hybrid Extended Kalman Filter

Majid Zohari, Mohamadreza Ahmadi, and Hamed Mojallali

Department of Electrical Engineering, Faculty of Engineering, University of Guilan, Rasht, Iran

E-mails: zohari@msc.guilan.ac.ir, mrezaahmadi@ieee.org, mojallali@guilan.ac.ir

Keywords: Air-to-Fuel Ratio Control; Hybrid Extended Kalman Filter; Dynamic Sliding Mode Control; Nonlinear Observer;

Abstract. The large modeling uncertainties and the nonlinearities associated with air manifold and fuel injection in spark ignition (SI) engines has given rise to difficulties in the task of designing an adequate controller for air-to-fuel ratio (AFR) control. Although sliding mode control approaches has been suggested, the inescapable time-delay between control action and measurement update results in chattering. This paper proposes the implementation of a nonlinear observer based control scheme incorporating the hybrid extended Kalman filter (HEKF) and the dynamic sliding mode control (DSMC). The results established upon the proposed methodology are given which demonstrate superior performance in terms of reducing the chattering magnitude.

Nomenclature

$\dot{m}_{ap}$	Air mass flow in cylinder (kg/s)
$\dot{m}_{at}$	Air mass flow past throttle plate (kg/s)
$\dot{m}_{f}$	Cylinder port fuel mass flow (kg/s)
$\dot{m}_{fv}$	Fuel vapor mass flow (kg/s)
$\dot{m}_{fi}$	Injected fuel mass flow (kg/s)
n	Crank shaft speed (Kilo revolution per minute)
p_a	Atmospheric pressure (1.013 bar)
T_a	Atmospheric temperature (Kelvins)
X_f	Fraction of $\dot{m}_{fi}$ that is deposited on manifold as fuel film
H_u	Fuel lower heating value (4.3×10^4 kJ/kg)
η_i	Indicated efficiency
p_i	Manifold pressure (bars)
T_i	Manifold temperature (Kelvins)
P_l	Pumping and friction power (kW)
P_b	Load Power (kW)
R	Gas constant (287×10^{-5} J.bar/kg.K.Pa)
I	Crank shaft load inertia (kg.m^2)
V_d	Engine displacement (liters)
V_i	Manifold+port passage volume (m^3)

Introduction

Owing to the ever increasing regulations on exhaust emissions, the AFR control has received overwhelming attention in literature [1-6]. A conventional method to meet the emission standards is to use a 3-way catalytic converter which simultaneously oxidizes and decreases the exhaust pollution. However, the catalyst is quite sensitive to the AFR, and it has been observed that the optimal catalyst performance is achieved when the AFR is maintained at its stoichiometric value at 14.67. Slight deviations from the stoichiometric value can lead to considerable increase in pollutant gas (e.g. HC, CO and NO_x) emission levels [6-10]. Thus, the goal of an apt control strategy should

be to strictly control the AFR to remain constant at 14.67. In addition, a candidate control approach should be robust since the engine could operate in different operating points, different environmental conditions, and with different aging history of components.

Technically, the overall AFR is controlled via the injection system. Hence, the controlling methods are focused on this section of the SI engine. Previous studies have shown that the sliding mode control (SMC) algorithm which is in accordance with the binary nature of the oxygen sensor signal stands as an outstanding option for fuel injection control. The main drawback of the SMC is the occurrence of chattering in the neighborhood of the sliding surface. This problem stems from the inevitable oxygen sensor time-delay and the measurement errors. The chattering problem limits the magnitude of the feedback gain; however, to satisfy the surface reaching condition, a specific quantity of gain is needed. In [9], the authors used adaptive neural networks for online estimation of physical parameters which led to the reduction of chattering. Ref. [10] suggests applying adaptive updating laws for two fueling parameters that describe the fuel flow into the cylinders, and a third parameter that describes the air flow into the cylinders. The adaptive updating laws have brought about the possibility to decrease the sliding mode gain thus shrinking the oscillation amplitude caused by chattering. [11] compares the performance of a globally linearizing control (GLC) method with that of a SMC. Noticeably, the SMC outperforms the GLC with regard to robustness properties.

To get around the problems caused by the uncertainties and nonlinearities of the overall model, sub-optimal filtering based algorithms can be exploited in order to estimate the process (ignition system) states from the noisy measurements. Following this trend, the EKF has been employed for state estimation in the system model [12-14].

In the proposed scheme in this paper, firstly the uncertain states such as the manifold temperature and pressure are estimated using the HEKF, subsequently based on the estimated states, the DSMC is applied to maintain the AFR in the desired level. Simulation results are included which validate the proposed control method's efficiency.

This paper is organized as follows. Section 2 describes the mean value engine model (MVEM) as implemented in this study. In section 3, the DSMC is outlined. The design of a nonlinear observer using the HEKF is delineated in section 4. The simulation results are provided in Section 5. The paper ends with conclusions in section 6.

Engine Model Description

Among the available internal combustion engine models available in open literature, the MVEM brought forward by Hendricks [15] is mathematically compact and can be readily parameterized for different engines. Therefore, our approach in this paper is also established upon the MVEM. In this study, the throttle opening angle α and the injected fuel mass flow $\dot{m}_{fi}$ are considered as the inputs and the AFR as the output of the model. The MVEM consists of three subsystems which are described next.

a) *Fueling system*: The fluid film flow model describes the dynamics of the fluid flow through the manifold. The fluid flow has two components: fuel vapor flow ($\dot{m}_{fv}$) and the fuel film flow ($\dot{m}_{ff}$). The overall inlet fuel flow ($\dot{m}_f$) is not measurable. The following equations describe the dynamics of the subsystem:

$$\dot{m}_{ff} = \frac{1}{\tau_f}\left(-\dot{m}_{ff} + X_f \dot{m}_{fi}\right) \tag{1.a}$$

$$\dot{m}_{fv} = (1 - X_f)\dot{m}_{fi} \tag{1.b}$$

$$\dot{m}_f = \dot{m}_{fv} + \dot{m}_{ff} \tag{1.c}$$

where τ_f is the fuel evaporation time constant which is both dependent on the engine type and operating conditions. [15] claims that these parameters can be computed as:

$$\tau_f = 1.35(-0.672n + 1.68)(p_i - 0.825)^2 + (-0.06n + 0.15) + 0.56 \tag{2.a}$$

$$X_f = -0.277 p_i - 0.055n + 0.68 \tag{2.b}$$

The normalized air-to-fuel ratio is denoted by

$$\lambda = \frac{\dot{m}_{ap}}{\beta \dot{m}_f} \tag{3}$$

where β signifies the stoichiometric ratio namely 14.67. It is worth noting that the time-delay associated with the fuel injection process should be considered. There are three major sources of delay: the sensor's measurement delay, the time-delay resulted from the distance between exhaust ports and sensor locations, and the physical delay regarding the fuel flow which is a consequence of the finite rate of evaporation of the fuel film on the inlet manifold and port walls [7,8,10].

b) *Crank shaft speed dynamics*: This sub-model is derived from energy conservation laws. The crank shaft speed is calculated by

$$\dot{n} = -\frac{1}{nI}\left(P_l(p_i, n) + P_b(n)\right) + \frac{1}{nI} H_u \eta_i(p_i, n, \lambda) \dot{m}_f(t - \tau_d) \tag{4}$$

where τ_d is the torque-injection delay.

c) *Air flow system*: The air mass passing through the manifold is represented by

$$\dot{p}_i = \frac{\kappa R}{V_i}\left(-\dot{m}_{ap} T_i + \dot{m}_{at} T_a\right) \tag{5.a}$$

$$\dot{T}_i = \frac{R T_i}{p_i V_i}\left[-\dot{m}_{ap}(\kappa - 1) T_i + \dot{m}_{at}(\kappa T_a - T_i)\right] \tag{5.b}$$

$$\dot{m}_{at}(\alpha, p_i) = m_{at1} \frac{p_a}{\sqrt{T_a}} \beta_1(\alpha) \beta_2(p_r) + m_{at0} \tag{5.c}$$

$$\dot{m}_{ap}(n, p_i) = \frac{V_d}{120 R T_i}(e_v . p_i) n \tag{5.d}$$

$$\beta_1(\alpha) = 1 - \cos(\alpha) - \frac{u_0^2}{2!} \tag{5.e}$$

$$p_r = p_i \Big/ p_a \tag{5.f}$$

$$\beta_2(p_r) = \begin{cases} \sqrt{1 - \left(\dfrac{p_r - p_c}{1 - p_c}\right)^2}, & \text{if } p_r \geq p_c \\ 1, & \text{if } p_r < p_c \end{cases} \tag{5.g}$$

in which m_{at0}, m_{at1}, u_0, and p_c are all constant values. κ denotes the ratio of the specific heats (1.4 for air). Moreover, instead of deriving a direct model for volumetric efficiency e_v, it is rather convenient to use $e_v . p_i$ which is called the normalized air charge. The normalized air charge is given by

$$(e_v . p_i) = s_i(n) p_i + y_i(n) \tag{6}$$

where both $s_i(n)$ and $y_i(n)$ are weak and positive functions of crank shaft speed and $y_i << s_i$.

AFR Control using The DSMC

The sliding surface is defined as [9, 10]:

$$S = \dot{m}_{ap} - \beta \dot{m}_f \tag{7}$$

To ensure that the sliding surface reaches the sliding surface $(S = 0)$ in a finite time, $\dot{m}_{fi}$ should be controlled such that the attraction condition is met

$$S\dot{S} \leq -k|S| \tag{8}$$

where k is a positive gain. In order to obtain the derivative of the sliding surface, one has to calculate $\ddot{m}_{ap}$ and $\ddot{m}_f$ in advance. The derivatives are determined using Eqs. (1.a-1.c) as follows:

$$\ddot{m}_{ap} = \frac{\partial \dot{m}_{ap}}{\partial p_i} \dot{p}_i + \frac{\partial \dot{m}_{ap}}{\partial n} \dot{n} \tag{9.a}$$

$$\ddot{m}_f = \ddot{m}_{fv} + \frac{1}{\tau_f}\left(\dot{m}_{fi} - \dot{m}_f\right) \tag{9.b}$$

Thus, using Eqs. (7), (9.a-9.b) we have

$$\dot{S} = -K_p T_i S + K_p\left(T_a \dot{m}_{at} - \beta T_i \dot{m}_f\right) + K_n \dot{n} - \beta\left[\ddot{m}_{fv} + \frac{1}{\tau_f}\left(\dot{m}_{fi} - \dot{m}_f\right)\right] \tag{10.a}$$

$$K_p = \frac{\partial \dot{m}_{ap}}{\partial p_i} \cdot \frac{\kappa R}{V_i} \tag{10.b}$$

$$K_n = \frac{\partial \dot{m}_{ap}}{\partial n} \tag{10.c}$$

The derivative of the control input $\dot{m}_{fi}(t)$ can be chosen as

$$\ddot{m}_{fi} = \frac{1}{\beta\left(1 - X_f\right)}\left[K_p\left(T_a \dot{m}_{at} - \beta T_i \dot{m}_f\right) + K_n \dot{n} - \frac{\beta}{\tau_f}\left(\dot{m}_{fi} - \dot{m}_f\right) + \eta\,\mathrm{sgn}\left(S(t - t_a)\right)\right] \tag{11}$$

Note that the term $\mathrm{sgn}(S(t-t_d))$ is the output of the binary oxygen sensor, where t_d denotes the sensor's measurement delay. Substituting (11) in (10) yields

$$\dot{S} = -K_p T_i S - \eta\,\mathrm{sgn}(S(t - t_d)) \tag{12}$$

The sliding criteria (8) is guaranteed as

$$\eta \geq \left|K_p T_i S\right| + k > \left|K_p T_i S\right| \tag{13}$$

State Estimation Via The HEKF

The nonlinear observer can be designed by considering the mathematical models for fuel injection system and the sensors. The system equations can be rewritten as follows

$$\begin{bmatrix} \dot{p}_i \\ \dot{T}_i \\ \dot{T}_{ms} \end{bmatrix} = \begin{bmatrix} \frac{\kappa R}{V_i}\left(-\dot{m}_{ap} T_i + \dot{m}_{at} T_a\right) \\ \frac{R T_i}{p_i V_i}\left[-\dot{m}_{ap}(\kappa - 1) T_i + \dot{m}_{at}(\kappa T_a - T_i)\right] \\ -\frac{1}{\tau_t}\left(T_{ms} - T_i\right) \end{bmatrix} + \begin{bmatrix} w_{p_i} \\ w_{T_i} \\ w_{T_{ms}} \end{bmatrix} \tag{14.a}$$

$$p_{mm} = p_i + v_{p_{mm}} \tag{14.b}$$

$$T_{mm} = T_{ms} + v_{T_{mm}} \tag{14.c}$$

where p_{mm} and T_{mm} are the measured manifold pressure and temperature, respectively. The state T_{ms} is associated with the temperature sensor with a time constant (τ_t) of 0.2s. Also, the vector $w = \left[w_{p_i}, w_{T_i}, w_{T_{ms}}\right]^T$ is a continuous-time Gaussian process noise with a covariance matrix of Q, and $v = \left[v_{p_{mm}}, v_{T_{mm}}\right]^T$ is a discrete-time Gaussian measurement noise with a covariance matrix of R_k such that Q and R_k are statistically independent. Note that Q and R_k are positive semi-definite and definite matrices, respectively. The system and measurement dynamics can be simplified as

$$\dot{x} = f(x,u) + w \tag{15.a}$$

$$z_k = H x_k + v_k \tag{15.b}$$

in which $x = \left[p_i, T_i, T_{ms}\right]^T$ represents the state vector, $u = \alpha$ is the input, $z = \left[p_{mm}, T_{mm}\right]^T$ is the measurement vector, and f consists of nonlinear functions given by (14.a). Based on the ignition system and sensor models, the HEKF estimation equations which are applied at each measurement time instance are given below [16]:

$$\dot{\hat{x}} = f(\hat{x},u) \tag{16.a}$$

$$\dot{P} = AP + PA^T + Q \tag{16.b}$$

$$A = \frac{\partial f(x,u)}{\partial x}\Big|_{x=\hat{x}} \tag{16.c}$$

where P is the error covariance matrix, A is the linearized system matrix, and $\hat{x}$ is the estimated state vector. The superscripts '+' and '-' represent a posterior and a prior state estimate, respectively. Then, the HEKF updating rules are utilized to calculate the corresponding Kalman gain, state estimates and error covariance matrix. The updating rules are cited below

$$K_k = P_k^- H^T \left(HP_k^- H^T + R_k\right)^{-1} \tag{17.a}$$

$$\hat{x}_k^+ = \hat{x}_k^- + K_k\left(z_k - H\hat{x}_k^-\right) \tag{17.b}$$

$$P_k^+ = \left(I - K_k H\right)P_k^-\left(I - K_k H\right)^T + K_k R_k K_k^T \tag{17.c}$$

wherein K_k is the Kalman gain at time instance k and I denotes the identity matrix.

Simulation Results

The results given in this section are derived from the MVEM model for a 1275cc engine which is investigated by Hendricks in [15]. The throttle angle changes are illustrated in Fig.1. It should be noted that the speed of throttle angle alterations are exaggerated and in a real case the variations are more gradual. Furthermore, a random signal with a uniform distribution between 0-0.2 degrees is added to throttle angle which accounts for model uncertainties or disturbances. In order to model the drive by wire (DBW) actuator with its controller, a second-order low pass filter with un-damped natural frequency of $76.9\ rad/\sec$ and a damping parameter of 0.675 is adopted. The filter output is considered as the actual throttle angle [12,13]. Besides, all of the system time-delays are taken into account during simulations.

The DSMC as described in section III is applied. The simulation results are depicted in Fig.2. As it is observed, there exist severe fluctuations around the stoichiometric value, and the algorithm's performance is not satisfactory. To overcome the control failure, the closed loop control scheme using the HEKF state estimator and the DSMC is implemented. Fig.3 shows both the estimated pressure and actual measured pressure signal. The estimated and measured temperature is displayed in Fig.4, as well. Accordingly, the HEKF is able to precisely approximate the manifold pressure and temperature in the presence of noisy and uncertain measurements. Crank shaft speed changes are portrayed in Fig.5. Finally, Fig.6 demonstrates the proposed algorithm's AFR control performance by incorporating HEKF, and DSMC. It is obvious that the chattering phenomenon which can lead to mechanical wear has been rigorously dwindled, and the AFR magnitude is maintained within $14.67 \pm 1\%$ except in instances where sudden transients of throttle angle signal are present. Another notable feature of the proposed algorithm is that despite abrupt changes in throttle angle, the AFR exhibits a relatively smooth response.

Summary

This paper considers the AFR control problem in SI engines. Firstly, the performance of the DSMC is examined and it is noticed that there exist considerable chattering oscillations. Then, a nonlinear observer established upon the HEKF is proposed. The functionality of the control approach based on the HEKF along with the DSMC is evaluated through simulations. The simulation results prove the proposed control scheme's capability to maintain the AFR in the desired range.

Refrences

[1] T. Huajin, L. Weng, Z.Y. Dong, and R. Yan , "Adaptive and Learning Control for SI Engine Model With Uncertainties", *IEEE/ASME Transactions on Mechatronics,* vol. 14, no. 1, pp. 93-104, Feb. 2009.

[2] L. Derong, H. Javaherian, O. Kovalenko, and T. Huang, "Adaptive Critic Learning Techniques for Engine Torque and Air-Fuel Ratio Control," IEEE *Transactions on Systems, Man, and Cybernetics, Part B: Cybernetics,* vol. 38, no. 4, pp. 988-993, Aug. 2008.

[3] D. Rupp and L. Guzzella, "Iterative Tuning of Internal Model Controllers With Application to Air/Fuel Ratio Control," *IEEE Transactions on Control Systems Technology,* vol. 18, no. 1, pp. 177-184, Jan. 2010.

[4] N. Cavina, E. Corti, and D. Moro, "Closed-loop individual cylinder air-fuel ratio control via UEGO signal spectral analysis," *Control Engineering Practic,* vol. 18, no. 11, pp. 1295-1306, Nov. 2010.

[5] K. R. Muske, J. C. P. Jones, and E. M. Franceschi., "Adaptive Analytical Model-Based Control for SI Engine Air-Fuel Ratio," *IEEE Transactions on Control Systems Technology ,* vol. 16, no. 4, pp. 763-768, July 2008.

[6] D. Rupp and L. Guzzella, "Adaptive internal model control with application to fueling control," *Control Engineering Practice,* vol. 18, no. 8, pp. 873-881, Aug. 2010.

[7] C. Manzie, M. Palaniswami, and H. Watson, "Gaussian networks for fuel injection control," *In Proceedings of the Institution of Mechanical Engineers, Part D, Journal of Automobile Engineering*, vol. 215, no. 10, pp. 1053–1068, 2001.

[8] C. Manzie, M. Palaniswami, D. Ralph, H. Watson, and X. Yi, "Model predictive control of a fuel injection system with a radial basis function network observer," *J. Dyn. Syst. Meas. Control Trans. ASME*, vol. 124, no. 4, pp. 648–658, Dec. 2002.

[9] S. W. Wang, and D. L. Yu, "Adaptive RBF network for parameter estimation and stable air-fuel ratio control," *Neural Networks*, vol. 21, no. 1, no. 1, pp. 102-112, Jan. 2008.

[10] J. S. Souder and J. K. Hedrick, "Adaptive sliding mode control of air–fuel ratio in internal combustion engines," *International Journal of Robust and Nonlinear Control*, vol.. 14, no. 6, pp. 525–541, April 2004.

[11] T. Huajin, L. Weng, D. Zhao Yang, and Y. Rui, "Engine control design using globally linearizing control and sliding mode," *Transactions of the institute of Measurement and Control*, vol. 32, no. 2. pp. 225-247, April 1, 2010.

[12] A. Chevailer, C. W. Vigild, and E. Hendricks, "Predicting the Port Air Mass Flow of SI Engines in Air/Fuel Ratio Control Applications", *SAE Technical Paper*, no. 2000-01-0260, 2000.

[13] A. Dutka, H. Javaherian, M. J. Grimble, "State-Dependent Kalman Filters for Robust Engine Control," in *Proc. of the 2006 American Control Conference*, Minneapolis, Minnesota, USA, June 14-16 2006.

[14] P. Anderson, "Air charge estimation in turbocharged spark ignition engines," Ph.D. dissertation, Dept. Elect. Eng., Linköping Univ., Linköping, Sweden, 2005.

[15] E. Hendricks, "A generic mean value engine model for spark ignition engines," in *Proc. 41st SIMS Simul. Conference: SIMS* 2000, Lyngby, Denmark, Sep. 18-19 2000.

[16] D. Simon, *Optimal State Estimation: Kalman, H infinity, and Nonlinear Approaches,* 1st ed. Wiley & Sons, Aug. 2006.

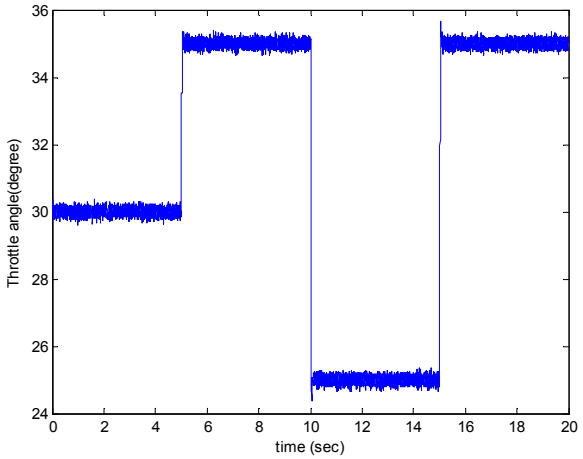

Fig. 1 Throttle angle variations

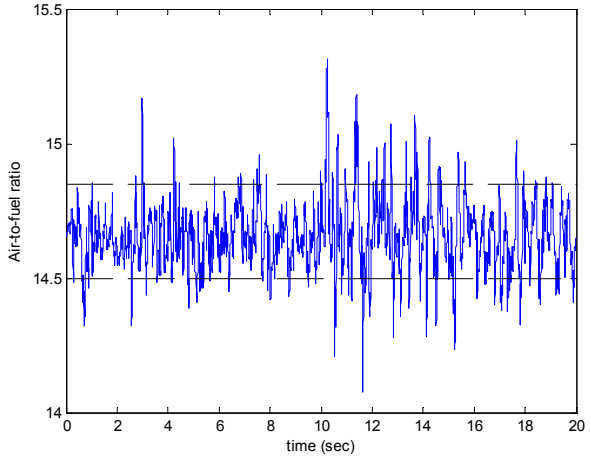

Fig.2 AFR control results using the DSMC without the nonlinear observer.

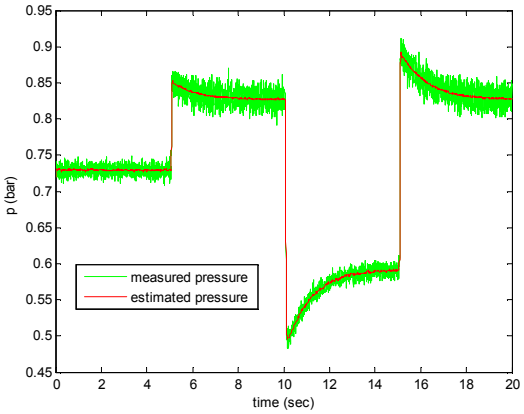

Fig. 3 The estimated $\hat{p}_i$ (red) and measured manifold pressure p_{mm} (green).

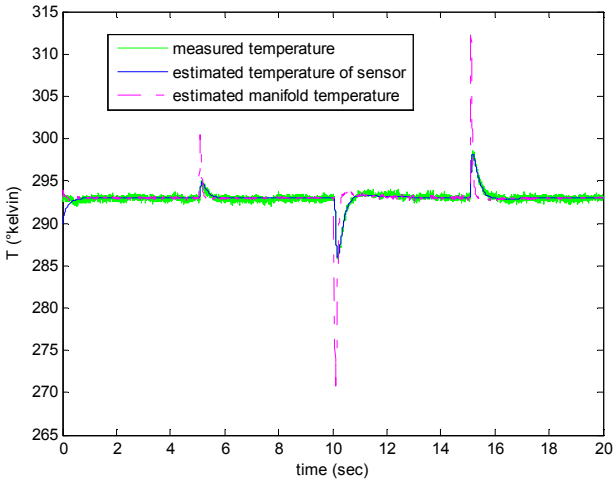

Fig.4 The estimated manifold temperature $\hat{T}_i$ (pink), the estimated temperature from sensor $\hat{T}_{ms}$ (blue), and the measured temperature T_{mm} (green).

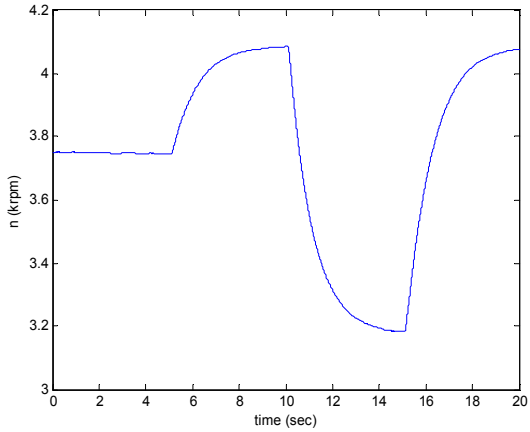

Fig. 5 Crank shaft speed variations n

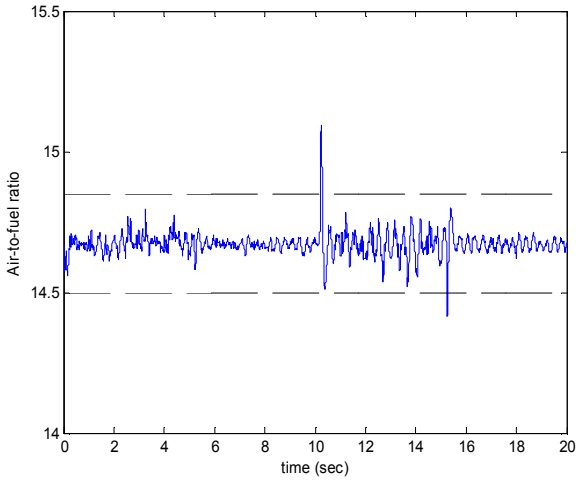

Fig. 6 The AFR control results when the DSMC is accompanied by a HEKF estimator.